Hindawi
Geofluids
Volume 2023, Article ID 6668841, 7 pages
https://doi.org/10.1155/2023/6668841

Research Article

Flow Field and Pressure Loss Characteristics at Rotary Drillstring Joints

Minghu Nie,[1] Yuchen Ye,[1] Zheng Wang,[1] Dandan Yuan,[1] Xingyi Wang,[2,3] and Kai Wei[2,3]

[1]*Engineering Technology Research Institute, PetroChina Xinjiang Oilfield Company, Karamay, Xinjiang 834000, China*
[2]*National Engineering Research Center for Oil & Gas Drilling and Completion Technology (Yangtze University), Wuhan 430100, China*
[3]*Hubei Key Laboratory of Oil and Gas Drilling and Production Engineering (Yangtze University), Hubei Province, Wuhan 430100, China*

Correspondence should be addressed to Kai Wei; weikai630@163.com

Received 2 December 2022; Revised 4 February 2023; Accepted 1 April 2023; Published 22 April 2023

Academic Editor: Peng Tan

A thorough understanding and accurate calculation of the annulus pressure losses are paramount to drilling design and construction. However, due to the influence of the drillstring rotation and the abrupt dimensional variation at the joint, it is difficult to calculate the pressure loss by theoretical analysis in the annulus at the drillstring joints. Considering the geometric nonlinearity of drillstring joints and the unsteady flow of annular fluid caused by pipe rotation, based on the turbulence model $k-\varepsilon$, the flow field characteristics demonstrate the annulus pressure losses at the drillstring joint are studied by numerical simulation. Simulation results indicate that drillstring rotation speed, annular gap, and eccentricity greatly influence flow field and pressure losses at drillstring joints. The annular pressure loss would increase with the decrease of the annular gap and eccentricity but decrease with the increase of the drillstring rotation rate. The investigation method and results would help guide the design of drilling hydraulic parameters.

1. Introduction

Hydraulic parameter design is essential for safe and efficient drilling, and capturing the flow field characteristics is the basis of the hydraulic parameters [1]. However, the flow in annuli is complex because of many variables, such as drillstring eccentricity, rotation, drilling mud rheology, and annular cross-section size. Many scholars have investigated fluid flow characteristics in the annulus and developed an empirical method for the annulus pressure loss [2, 3]. However, the annular flow passage at the drillstring joints has a remarkable characteristic of abrupt dimensional variation, resulting in a sharp change area of the flow cross-section and apparent pressure loss. Experimental results and field measurements have also confirmed this conclusion. In general, ignoring these pressure losses makes little difference in terms of shallow or medium deep wells, but in ultradeep wells or slim-hole wells, these local pressure losses will produce a cumulative effect with the increase of well depth. In addition, the rotation of the drillstring makes the flow field characteristics at the joint more complex, which significantly impacts the pressure loss.

Accurate estimation of frictional pressure loss in the annulus is essential for well control. Many investigators studied the pressure losses in the annuli over the years. For example, Hansen and Sterri [4] found experimentally that the frictional pressure loss in an annulus increase with high rotation rates for low-viscosity fluids and decreases with rotation for high-viscosity shear-thinning fluids. Ahmed and Miska [5] conducted experiments and theoretical analysis of helical flows in concentric annuli meanwhile presented a reliable hydraulic model that accounts for the effect of pipe rotation in annular pressure loss calculation. Enfis et al. [6] believed that the change in the annular gap would impact annular pressure loss. They regarded the drillstring joints as a part with different pipe sizes and built a simple model to solve the calculation model of pressure losses caused by the drillstring joints. Because the model ignores the influence of the outlet and inlet, the pressure loss of the whole drillstring joint is smaller than the actual situation. Saasen [7] investigated the effects of drillstring rotation, drilling mud rheology, and annular gap on annular pressure losses. The results showed that the drillstring rotation creates unstable flow and sometimes turbulence in the annulus even without axial flow. Erge et al. [8] established an annular pressure loss prediction model considering drillstring rotation, eccentricity, and buckling. Perez-Tellez et al. [9] proposed a comprehensive mechanism model suitable for underbalanced drilling, improving the wellbore pressure prediction accuracy. With the development of computational methods such as the finite element method (FEM), the finite difference method (FDM), and the finite volume method (FVM), it becomes possible to master the characteristics of the flow field by computer simulation technology [10, 11]. Many scholars apply the computational fluid dynamics method to study the flow around the drillstring joint [12–14]. The simulation results show that the annulus pressure losses depend heavily on the drilling mud rheology, axial flow rate, drill pipe rotational rate, and annulus gap. However, there is less relevant research on annulus pressure losses induced by the rotary drillstring joints. Therefore, it is necessary to study the characteristics of the flow field and the influencing factors of pressure loss at the drillstring joints under the rotating condition to guide the optimal design of hydraulic parameters.

In order to reveal the effects of drillstring joint rotation on the annulus pressure loss, we performed three types of CFD simulations (drilling rotation, eccentricity, and annular gap) to demonstrate the flow field characteristics and the annulus pressure losses at the drillstring joint. The investigation method and results would help guide the design of drilling hydraulic parameters.

2. Construction of Annular Pressure Loss Simulation Model for Rotary Drillstring Joint

The drillstring is the general term for all the pipes or tools below the swivel and above the drilling bit in rotary drilling, mainly composed of TDS, drill pipe, drill collars, tool joints, stabilizers, and other components [15]. Usually, the drillstring is not a whole pipe but composed of many pipes connected by tool joints. Figure 1 shows the structure diagram of the drillstring joint.

The fluid flow at the drillstring joint is a three-dimensional eccentric multiphase turbulent flow affected by the drillstring rotation. In order to reveal the characteristics of the complex flow field at the rotary drillstring joint and grasp the influencing factors and rules of the annulus pressure loss, we made the following assumptions when building the simulation model.

(1) The drilling fluid flow in the annuli is steady and satisfies the Navier-Stokes equation

(2) The fluid is regarded as an incompressible homogeneous fluid and satisfies the Herschel-Bulkley model

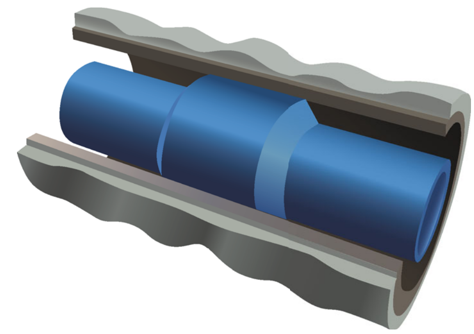

Figure 1: Geometry of the drillstring joint.

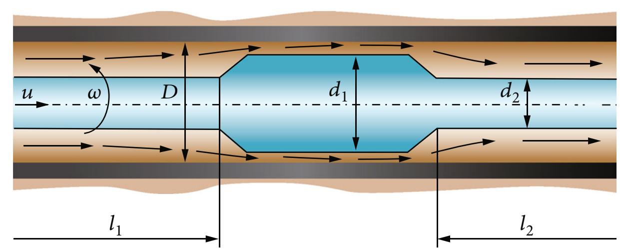

Figure 2: Geometry of the flow field outside the drillstring joint.

(3) Ignore the orbital motion and only consider the drillstring rotation of the drillstring itself

(4) Without wellbore diameter variation

2.1. Physical Model. According to the structural characteristics of the drillstring joint and the annulus working condition, assuming that the annulus outer diameter (wellbore wall or casing) is D, the outer diameter of the drillstring joint is d_1, and the outer diameter of the drillstring is d_2. Furthermore, to eliminate the influence of the inlet and outlet on turbulent flow, the upper-end and the lower-end length of the joint are l_1 and l_2, respectively. Figure 2 shows the geometry of the flow field outside the drillstring joint.

2.2. Mathematical Model. Most current drilling mud shows highly non-Newtonian behavior, which is practically well-explained by the Herschel-Bulkley model [16]. The Herschel-Bulkley model is given by

$$\tau = \tau_y + K\dot{\gamma}^n, \tag{1}$$

where τ is the shear stress of the drilling fluid, $\dot{\gamma}$ is the shear rate of the drilling fluid, K is the consistency index of the drilling fluid, and n is the flow behavior index of the drilling fluid.

The selection of the turbulence model is of great significance to numerical simulation. A suitable turbulence model can accelerate the convergence of calculation results and improve simulation accuracy, so we adopt a realizable turbulence model $k-\varepsilon$ in this paper (as shown in Equation (2)),

Table 1: The main CFD model parameters.

Parameters	Value	Parameters	Value
Mixture type	Fluid-solid mixture	Solid content (%)	15
Fluid density (g/cm^3)	1.5	Fluid viscosity (mPa·s)	25
Inner diameter of casing/borehole D (mm)	215.9	Joint lower length l_2 (mm)	500
Outer diameter of the joint d_1 (mm)	146.1	Inlet mean velocity u_{in} (m/s)	0.5, 1.0, 1.5, 2.0
Outer diameter of the drillstring d_2 (mm)	101.6114.3127.0 139.7 168.3	Drillstring eccentricity	0 ~ 0.8
Joint upper length l_1 (mm)	500	Rotational rate w (RPM)	0, 30, 60, 90, 120

which applies to the calculation of complex flows with separate or secondary flows [17].

$$\begin{cases} \dfrac{\partial(\rho k)}{\partial t} + \dfrac{\partial\left(\rho k \vec{u}_i\right)}{\partial x_i} = \dfrac{\partial}{\partial x_j}\left[\left(\mu + \dfrac{\vec{\mu}_t}{\sigma_k}\right)\dfrac{\partial k}{\partial x_j}\right] + G_k + G_b - \rho\varepsilon - Y_m + S_k, \\ \dfrac{\partial(\rho \varepsilon)}{\partial t} + \dfrac{\partial\left(\rho \varepsilon \vec{u}_i\right)}{\partial x_i} = \dfrac{\partial}{\partial x_j}\left[\left(\mu + \dfrac{\vec{\mu}_t}{\sigma_\varepsilon}\right)\dfrac{\partial \varepsilon}{\partial x_j}\right] + C_{1\varepsilon}\dfrac{\varepsilon}{k}\left(G_k + C_{3\varepsilon}G_b\right) - C_{2\varepsilon}\rho\dfrac{\varepsilon^2}{k} + S_\varepsilon, \end{cases} \quad (2)$$

where ρ is the drilling mud density; x_i/x_j is the coordinate component; ε is the turbulent dissipation rate; μ is the drilling mud viscosity; G_k is the turbulent kinetic energy caused by mean velocity gradient; G_b is the turbulent kinetic energy generated by buoyancy; Y_m is the contribution of compressible turbulence pulsation to the total dissipation rate; $C_{1\varepsilon}$, $C_{2\varepsilon}$, and $C_{3\varepsilon}$ are empirical constants; σ_k and σ_ε are Prandtl number of turbulent kinetic energy and dissipation rate; and S_k and S_ε are user-defined source item.

2.3. Solution Conditions

(1) Initial conditions

During the actual drilling process, the annulus between casing and drillstring is filled with a mixture of cuttings and drilling fluid. The cuttings' mass flow rate is about 15% of the mass flow rate of the drilling mud. Because the annular interface is in contact with the surface atmosphere, the initial pressure and temperature can be set to atmospheric pressure p_0 and atmospheric temperature T_0, respectively.

(2) Boundary condition

The upper end of the model is the outlet, which is set as the free outlet pressure boundary and equal to atmospheric pressure p_0. The lower end is the inlet boundary and is set as the speed inlet:

$$u_{in} = \frac{Q}{A_c}, \quad (3)$$

where u_{in} is the mean velocity, Q is the flow rate, and A_c is the entrance section area.

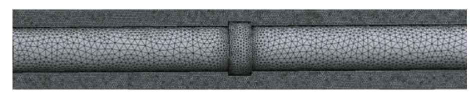

Figure 3: Mesh grid model of the drillstring joint.

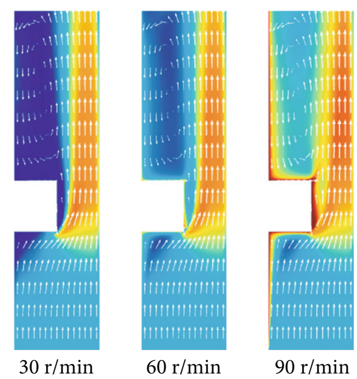

Figure 4: Flow field distribution at joint at different drillstring rotational rate.

2.4. Computational Fluid Dynamics Simulation (CFD). Due to the complex characteristics of the flow field at the rotary drillstring joint, we performed numerous CFD simulations to obtain the results of the solution for the mathematical model presented aforementioned. Table 1 shows the main model parameters for the CFD simulations, which are often used in drilling practices [15, 18].

In order to ensure the accuracy and efficiency of CFD simulation, it is necessary to reduce the number of elements as much as possible while ensuring finer grid resolution. Therefore, we divide the flow field region into three parts for mesh generation: the upstream annulus, the joint annulus, and the downstream annulus. Then, mesh the upstream and downstream annulus by structure hexahedral elements. Mesh the joint annulus by unstructured hexahedral elements and connect each part by the interface elements. In addition, we refined the mesh grid at the drillstring joints to ensure the accuracy and efficiency of CFD simulations. Figure 3 shows the mesh grid of the finite element model.

3. Results and Discussions

3.1. Flow Field Characteristics. We can obtain the flow field at the joint under different drillstring rotational rates. For

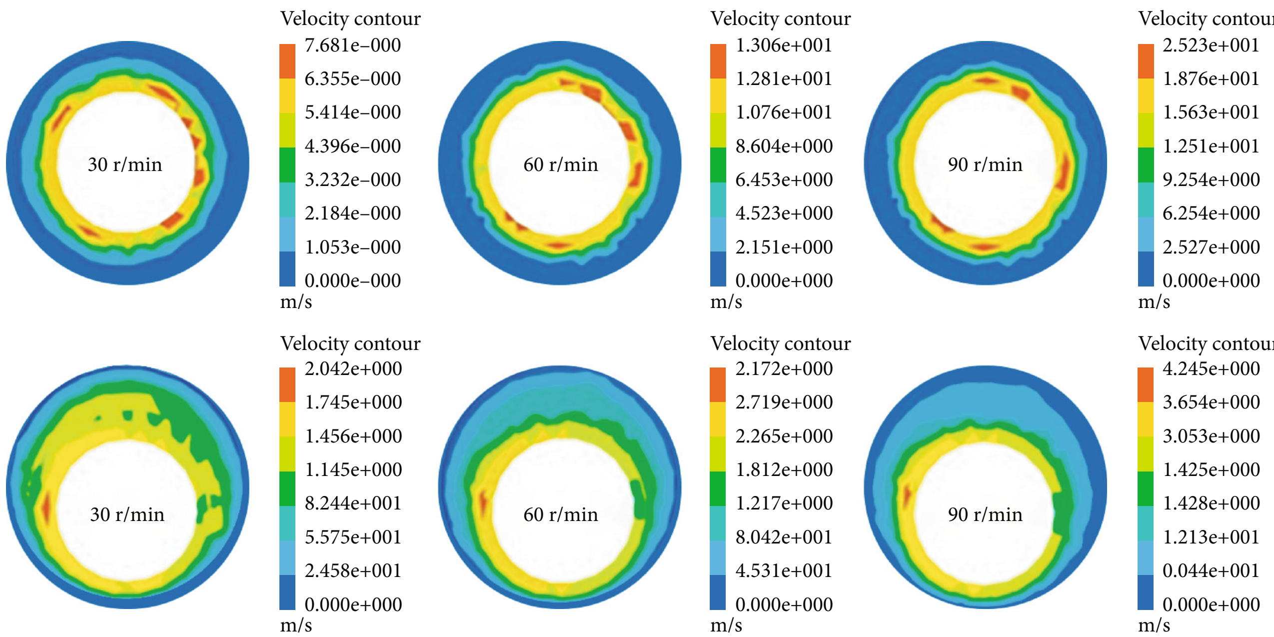

Figure 5: Comparison of the velocity in concentric and eccentric annuli with different rotational rates.

example, Figure 4 shows the flow field when the annular gap is 57.15 mm, and the drillstring rotational rate are 30 r/min, 60 r/min, and 90 r/min, respectively.

As shown in Figure 4, the velocity of drilling fluid flowing into the joint area will increase sharply under the influence of flow cross-sectional area decrease. However, a vortex would form downstream when the drilling fluid flows out of the joint under the influence of the abrupt flow cross-sectional area increases below the drillstring joint. The formation, operation, and splitting of the vortex body will strengthen the relative motion among the microgroups of the drilling fluid, promote the redistribution of the flow rate, and cause the vortex energy consumption, resulting in an enormous local pressure loss. Moreover, the joint rotation will intensify the vortex's formation, leading to a further increase of pressure loss.

In addition, the eccentricity also influences annular flow field around the drillsting joints. For example, Figure 5 shows the distribution of the annular flow field when the eccentricity is 0 and 0.3, respectively.

As shown in Figure 5, a flow core area of drilling fluid exists in both concentric and eccentric annulus. With the increase of the drillstring rotational rate, the annular flow rate increases because drilling mud is a Herschel-Bulkley law fluid with shear thinning. The fluid viscosity decreases with the rotational rate and annular axial velocity increase. In the eccentric annulus, the narrow gap on the lower side has more significant fluid resistance, and the drilling fluid flows to the wide gap on the opposite side first. The drillstring rotation slightly influences the fluid interface at the joint. As the drillstring rotational rate increases, the drilling fluid in the annulus will generate circumferential helical flow, driving the drilling fluid in the wide gap into the narrow gap and constantly washing the drilling fluid in the narrow gap to avoid fluid stagnation.

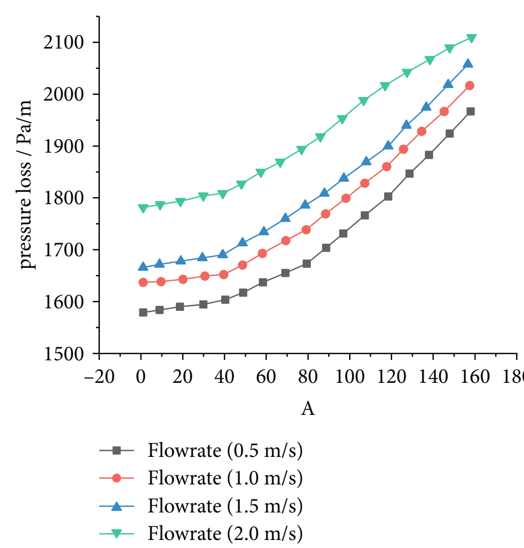

Figure 6: Effect of rotation on the pressure loss with various flowrates.

As shown from the flow field distribution of the above numerical simulation, the drillstring rotation rate, annular gap, and eccentricity greatly influence the drilling fluid flow at the drillstring joint. Therefore, these three parameters' influence on the joint's fluid pressure loss was simulated and analyzed.

3.2. Drillstring Rotation. A plot of pressure losses versus the rotational rate at the drillstring joint was analyzed, as shown in Figure 6. In addition, the inlet flow rate is 0.5 m/s, 1.0 m/s, 1.5 m/s, and 2.0 m/s, respectively.

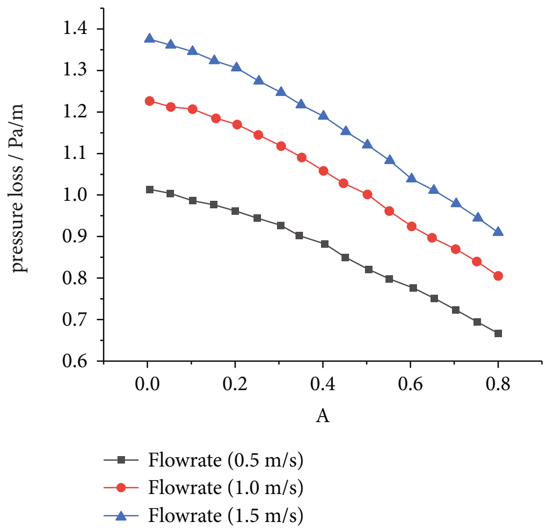

FIGURE 7: Effect of eccentricity on the pressure loss with various flowrates.

As shown in Figure 6, the fluid pressure loss increases significantly with the drillstring rotational rate. The reason is that the fluid disturbance inertia at the rotating joint will form significant viscous resistance, resulting in increased fluid resistance. Therefore, neglecting the drillstring rotation will inevitably form a significant deviation in the hydraulic calculation, which will bring certain risks to drilling design and construction.

3.3. Drillstring Eccentricity. Figure 7 shows the variation law of fluid pressure loss at the drillstring joint with drillstring varied when the inlet flow rate is 0.5 m/s, 1.0 m/s, 1.5 m/s, and 2.0 m/s, respectively.

As shown in Figure 7, under any annular flowrate condition, drill pipe eccentricity would reduce annular pressure loss along the joint. The basic reason is that with the increase of eccentricity, although the flow cross-sectional area in some eccentric annuli increases and the pressure lose decreases, the flow velocity in the narrow eccentric annuli is more seriously affected by the rheological properties of the liquid, resulting in a downward trend of the pressure loss in the upstream and downstream sections of the joint as a whole.

3.4. Annular Gap. Figure 8 shows the variation law of annulus pressure loss at the drillstring joint with gap width when the inlet flow rate is 0.5 m/s, 1.0 m/s, 1.5 m/s, and 2.0 m/s, respectively.

As shown in Figure 8, the annulus pressure loss increases rapidly as the gap width decreases. As the gap width decreases, the boundary layer effect between the drillstring outer wall and the wellbore's inner wall becomes more apparent, increasing the annulus pressure loss.

4. Conclusions

It is challenging to calculate annular pressure losses by theoretical analysis due to factors such as flow cross-sectional area decrease, flow cross-sectional area increases, and rotation of the drillstring joint. In this paper, we establishes a three-dimensional CFD model of the drillstring joints to analyze the influences of drillstring rotation, annular gap, and eccentricity on the flow field and pressure losses at the drillstring joints and reveal their influence law. As a result, we can obtain the following conclusions from the investigation:

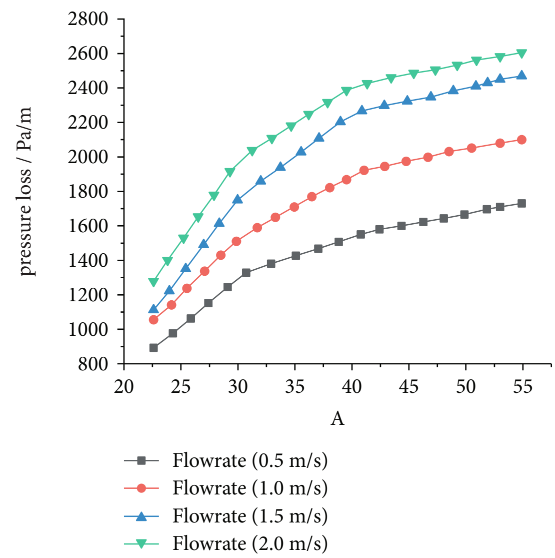

FIGURE 8: Effect of gap width on the pressure loss with various flowrates.

(1) Under the influence of the drillstring joint, the decrease of flow cross-sectional area would increase the drilling fluid velocity, and the abrupt flow cross-sectional area would create turbulent areas downstream of the joint, which results in a significant pressure loss between the upstream and downstream of the joint. In addition, the joint rotation and eccentricity will intensify the vortex's formation, further increasing the pressure losses

(2) Drillstring rotation speed, annular gap, and eccentricity greatly influence flow field and pressure losses at drillstring joints. Simulation results indicate that the annular pressure loss would increase with the decrease of the annular gap and eccentricity but decrease with the increase of the drillstring rotation rate

(3) The CFD simulations are effective in studying the annulus pressure loss at the rotary drillstring joint, which is not conducive to field engineering applications for its computationally demanding and long runtimes. Therefore, in the follow-up study, we would establish a multiparameter coupling model of drillstring joint pressure losses based on the current calculation model of pressure losses at the sudden expansion and contraction, which would consider factors such as drill pipe rotation, annular gap, and eccentricity. This would be very convenient for field application

Nomenclature

D: The inner diameter of the casing/borehole, m
d_1: The outer diameter of the drillstring, m
d_2: The outer diameter of the joint, m
l_1: Joint upper length, m
l_2: Joint lower length, m
A_c: The entrance section area, m^2
Q: The flow rate, m^3/s
ρ: The drilling mud density, kg/m^3
μ: The drilling mud viscosity, Pa·s
τ: The shear stress of the drilling mud, Pa
$\dot{\gamma}$: The shear rate of the drilling mud, 1/s
K: The consistency index of the drilling mud
n: The flow-behavior index of the drilling mud
u_{in}: The mean velocity, m/s
w: Rotational rate, RPM
x_i,x_j: The coordinate component
ε: The turbulent dissipation rate
G_k: The discrete phase generated by turbulent kinetic energy caused by mean velocity gradient, J
G_b: The turbulent kinetic energy generated by buoyancy, J
Y_m: The contribution of compressible turbulence pulsation to the total dissipation rate
$C_{1\varepsilon}$,$C_{2\varepsilon}$,$C_{3\varepsilon}$: Empirical constants
σ_k,σ_ε: Prandtl number of turbulent kinetic energy and dissipation rate
S_k, S_ε: User-defined source item.

Data Availability

The data supporting the findings of this study are available within the article.

Conflicts of Interest

The authors declare that they have no known competing financial interests or personal relationships that could have appeared to influence the work reported in this paper.

Authors' Contributions

Minghu Nie was involved in the conceptualization and methodology. Yuchen Ye was involved in the investigation and supervision. Zheng Wang was involved in the analysis of data. Dandan Yuan was involved in the data collection. Xingyi Wang was involved in the numerical simulation. Kai Wei was involved in the writing—reviewing the original draft.

Acknowledgments

This work was supported by a grant from the PetroChina Major Subject (2019E-2605).

References

[1] M. S. Ramsey, *Practical Wellbore Hydraulics and Hole Cleaning: Unlock faster, more Efficient, and Trouble-Free Drilling Operations*, Gulf Professional Publishing, 2019.

[2] A. A. Almabrok, A. M. Aliyu, Y. D. Baba et al., "A comparative analysis of upward and downward pressure gradient behaviour in vertical gas-liquid two-phase flows in a large diameter pipe facility," in *SPE Nigeria Annual International Conference and Exhibition*, Victoria Island, Lagos, Nigeria, 2020.

[3] U. Cartalos and D. Dupuis, "An analysis accounting for the combined effect of drillstring rotation and eccentricity on pressure losses in slimhole drilling," in *SPE/IADC Drilling Conference*, Amsterdam, Netherlands, 1993.

[4] S. A. Hansen and N. Sterri, "Drill pipe rotation effects on frictional pressure losses in slim annuli," in *SPE Annual Technical Conference and Exhibition*, Dallas, Texas, 1995.

[5] R. M. Ahmed and S. Z. Miska, "Experimental study and modeling of yield power-law fluid flow in annuli with drillpipe rotation," in *IADC/SPE Drilling Conference*, Orlando, Florida, USA, 2008.

[6] M. S. Enfis, R. M. Ahmed, and A. Saasen, "The hydraulic effect of tool-joint on annular pressure loss," in *Spe Production & Operations Symposium*, Oklahoma City, Oklahoma, USA, 2011.

[7] A. Saasen, "Annular frictional pressure losses during drilling—predicting the effect of drillstring rotation," *Journal of Energy Resources Technology*, vol. 136, no. 3, 2014.

[8] O. Erge, M. E. Ozbayoglu, S. Z. Miska et al., "Effect of drillstring deflection and rotary speed on annular frictional pressure losses," *Journal of Energy Resources Technology*, vol. 136, no. 4, 2014.

[9] C. Perez-Tellez, J. R. Smith, and J. K. Edwards, "A new comprehensive, mechanistic model for underbalanced drilling improves wellbore pressure predictions," in *SPE International Petroleum Conference and Exhibition in Mexico*, Villahermosa, Mexico, 2002.

[10] L. Huang, R. He, Z. Yang et al., "Exploring hydraulic fracture behavior in glutenite formation with strong heterogeneity and variable lithology based on DEM simulation," *Engineering Fracture Mechanics*, vol. 278, article 109020, 2023.

[11] P. Tan, H. Pang, R. Zhang et al., "Experimental investigation into hydraulic fracture geometry and proppant migration characteristics for southeastern Sichuan deep shale reservoirs," *Journal of Petroleum Science and Engineering*, vol. 184, article 106517, 2020.

[12] F. Behzadi and J. C. Newman III, "An exact source-term balancing scheme on the finite element solution of shallow water equations," *Computer Methods in Applied Mechanics and Engineering*, vol. 359, article 112662, 2020.

[13] R. Ershadnia, M. A. Amooie, R. Shams et al., "Non-Newtonian fluid flow dynamics in rotating annular media: physics-based and data-driven modeling," *Journal of Petroleum Science and Engineering*, vol. 185, article 106641, 2020.

[14] O. F. J. Meuric, T. W. Chiu, R. J. Wakeman, and K. A. Fisher, "A numerical study of helical flow of generalised Newtonian fluids in eccentric annuli," *Strojnicky Casopis*, vol. 48, pp. 363–373, 1997.

[15] R. F. Mitchell and S. Z. Miska, *Fundamentals of Drilling Engineering*, Society of Petroleum Engineers, 11 edition, 2011.

[16] P. Saramito, "A new elastoviscoplastic model based on the Herschel-Bulkley viscoplastic model," *Journal of Non-Newtonian Fluid Mechanics*, vol. 158, no. 1-3, pp. 154–161, 2009.

[17] M. M. K. Dawood, M. A. Teamah, A. I. Shehata, and T. Nabil, "Experimental and numerical investigation of turbulent natural convection between two horizontal concentric cylinders at different axis ratios and orientation angles," *Experimental Thermal and Fluid Science*, vol. 91, pp. 20–34, 2018.

[18] P. E. Clark, "Drilling mud rheology and the API recommended measurements," in *SPE Production Operations Symposium*, Oklahoma City, Oklahoma, 1995.